TELKOMNIKA, Vol.13, No.3, September 2015, pp. 767~775
ISSN: 1693-6930, accredited A by DIKTI, Decree No: 58/DIKTI/Kep/2013
DOI: 10.12928/TELKOMNIKA.v13i3.2093

Simulation Analysis of Interface Circuits for Piezoelectric Energy Harvesting with Damped Sinusoidal Signals and Random Signals

Shuai Pang, Wenbin Li*, Jiangming Kan
School of Technology, Beijing Forestry University, Beijing, 100083, China
*Corresponding author, e-mail: leewb@bjfu.edu.cn

Abstract

Various interface circuits for collecting the energy of piezoelectric cantilever beams have been widely investigated. Such circuits include the standard interface, series synchronized switch harvesting interface circuit, parallel synchronized switch harvesting interface, synchronized charge extraction interface, and others. Most studies focus on the performance of different interface circuits with standard sinusoidal excitations. However, in real situations where constant harmonic vibrations are not present, the equivalent voltage from piezoelectric cantilever beams with excitations is not necessarily sinusoidal. In the present study, a simulation analysis of four different interface circuits with signal sources that are both damped sinusoidal and random was performed using Matlab and PSpice. The results show that the interface circuits have improved performance under low load resistance values with damped sinusoidal signal. In addition, the parallel and series synchronized switch harvesting interface circuits may perform well in collecting piezoelectric energy with random excitations.

Keywords: *piezoelectric energy harvesting, interface circuit, damped sinusoidal signal, random signal, SLPS*

1. Introduction

Micro-energy harvesting has been widely studied because of the development of wireless sensor networks. Various energy harvesting techniques, such as solar energy, thermal energy, and vibration energy have been investigated to eliminate dependence on batteries or wires [1-5]. The electromagnetic, electrostatic, and piezoelectric transition mechanisms are the main methods for harvesting vibration energy. In particular, piezoelectric vibration energy harvesting has received significant attention for its high power density, simple structure, and ability to operate without producing pollution [6].

A piezoelectric energy harvesting system mainly consists of a mechanical structure and interface circuits. With regard to the mechanical structures in such systems, cantilever beams with patches of piezoelectric materials have been extensively investigated [7, 8]. The performance of the energy generated by piezoelectric elements with harmonic excitations has been studied widely. Recently, flow-induced piezoelectric energy harvesting has gained much attention. Some of the trends in piezoelectric energy harvesting are multi-directional wideband technology [9] and flow-induced or impact-induced piezoelectric energy harvesting [10]. In these systems, the electricity generated by piezoelectric cantilever beams is not sinusoidal. Meanwhile, the mechanical structures for collecting multi-direction energy and flow-induced piezoelectric energy have been widely investigated. Experiments on many mechanical structures under different conditions have been performed to evaluate the performance of different structures. With regard to interface circuits, the standard interface circuit, series synchronized switch harvesting interface circuit (S-SSHI), parallel synchronized switch harvesting interface circuit (P-SSHI), and synchronized charge extraction interface circuit (SCE) have been analyzed in detail, and all involve standard sinusoidal equivalent sources [11-13]. However, the performance of different interface circuits with a non-standard sinusoidal equivalent source has been minimally investigated. Many experiments have been performed in ideal laboratory environments where piezoelectric elements were subjected to harmonic excitations; thus, numerous analyses involving sinusoidal signals have been made. An exciter

Received April 23, 2015; Revised June 29, 2015; Accepted July 12, 2015

can generate sinusoidal excitations on piezoelectric elements. However, in practical experiments without exciters, the acting force on piezoelectric elements have not been harmonic; thus, the voltage generated by the elements has not been sinusoidal.

Modeling for piezoelectric energy harvesting has been studied to convert complex mechanical fields to purely electrical fields. The equivalent circuit modeling used in this paper is based on [14], which avoids a complicated derivation for theoretical modeling. Also, a simulation analysis of four different interface circuits with non-standard sinusoidal equivalents was performed using Matlab and PSpice. For the equivalent voltage source in the model, the damped sinusoidal signal source and random signal source used were based on the experimental voltage in [15] and [16]. To present the framework for the simulation analysis, we introduce the basics of energy harvesting, including the equivalent circuit model, four passive interface circuits, and non-standard sinusoidal signals. We then present the simulation method to analyze the performance of the four interface circuits using Matlab and PSpice, as well as the results of the simulation. Finally, the paper is summarized in the conclusion section.

2. Energy Harvesting Basics

2.1. Equivalent Circuit Model for a Piezoelectric Energy Harvesting System

The vibration energy harvester can be modeled as a system with a single degree of freedom, as shown in Figure 1 [11]. The system is composed of mass (*M*), total stiffness (*K*), and damping element (*C*). The equation of motion for the system is given by (1).

$$M\ddot{u} + C\dot{u} + Ku = F - \alpha v_p \quad (1)$$

Where *F* is the excitation force, *u* is the displacement of the piezoelectric structure, α is the force factor of the piezoelectric element, and v_p is the generated voltage from the piezoelectric element.

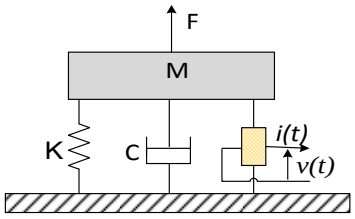

Figure 1. Equivalent model of a piezoelectric energy harvesting device

A piezoelectric cantilever beam can be modeled as a sinusoidal current ($i_p(t)$) in parallel with a capacitor (C_p) when a harmonic motion is functioning on the beam, as shown in Figure 2. The magnitude of $i_p(t)$ is I_p, which varies with the mechanical excitation level of the piezoelectric harvester but is assumed to be relatively constant regardless of external loading. Equivalent current $i_p(t)$ is given in (2) [14].

$$i_p(t) = I_p \sin(wt) \quad (2)$$

Where w is the excitation angular frequency of the piezoelectric energy harvester. Magnitude V_p of open circuit voltage *v(t)* is given in (3).

$$V_p = \frac{I_p}{wC_p} \quad (3)$$

In this paper, $i_p(t)$ is not considered as a sinusoidal current source but as a damped sinusoidal signal source and as a random signal source separately. Thus, open circuit voltage

v(t), which is generated from the piezoelectric energy harvester, becomes a damped sinusoidal voltage and a random voltage.

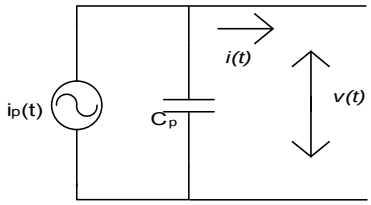

Figure 2. Equivalent circuit model of a piezoelectric energy harvester

2.2. Four Self-Powered Interface Circuits

A standard interface circuit [17] is composed of a rectifier and a filter capacitor, together with a supplied system (Rload), as shown in Figure 3. If excitation force *F* applied to the piezoelectric element is assumed to be purely sinusoidal, then mechanical displacement *u* would be sinusoidal. The generated voltage of the piezoelectric element under an open circuit condition would then be sinusoidal as well. However, when the piezoelectric element is connected to an interface circuit, the waveform of the piezoelectric voltage would be changed. Once the absolute value of *v(t)* is greater than the rectified voltage, the rectifier diodes are conducted and the charges accumulated on the piezoelectric element are transferred to capacitor Crect and load resistance Rload. The output power from the standard interface circuit can be expressed as (4):

$$P_{(\text{standard})} = 4f\left(\alpha u_M V_{rect} - C_p V^2_{rect}\right) \tag{4}$$

Where *f* is the resonance frequency of the system and u_M is the maximal displacement amplitude. The maximal harvested power under a given displacement magnitude is given by (5) with the optimal resistance value given by (6).

$$P_{(\text{standard})\max} = \frac{f\alpha^2 u_M{}^2}{C_p} \tag{5}$$

$$R_{opt} = \frac{1}{4fC_p} \tag{6}$$

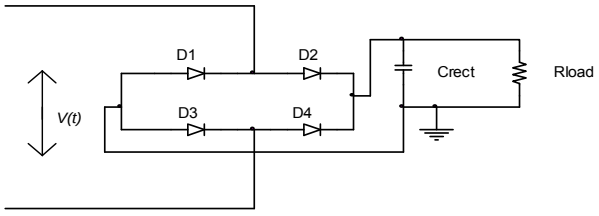

Figure 3. Block diagram of a standard interface circuit

Figures 4-6 show the block diagrams of the S-SSHI, P-SSHI, and SCE interface circuits, respectively [11, 18]. An electronic breaker circuit for switching on extreme values is used, which consists of an envelope detector, a comparator, and a digital switch [19]. The electronic breaker circuit for switching on maxima is shown in Figure 7. A minima switch control topology is conducted in a similar mode, with opposite polarities of diodes and transistors, as shown in Figure 7. Further information on the working principle can be found in [11-12], [18-19].

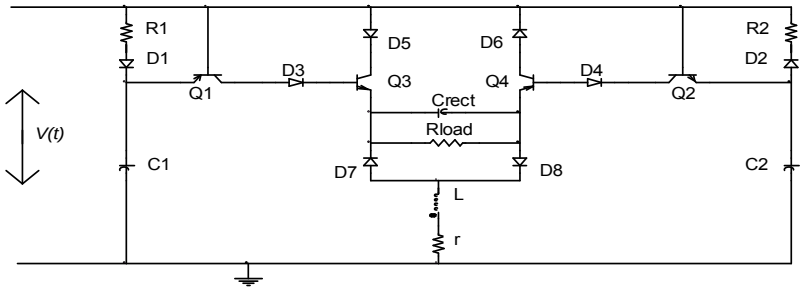

Figure 4. Block diagram of a S-SSHI interface circuit

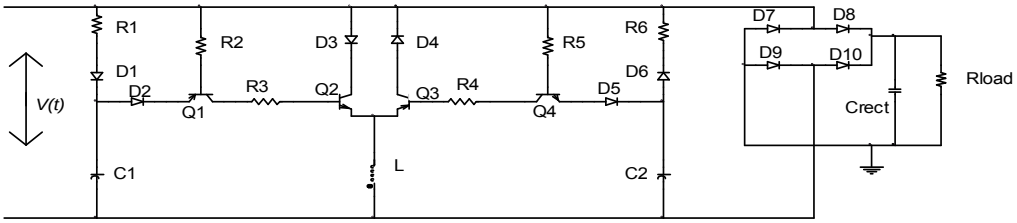

Figure 5. Block diagram of a P-SSHI interface circuit

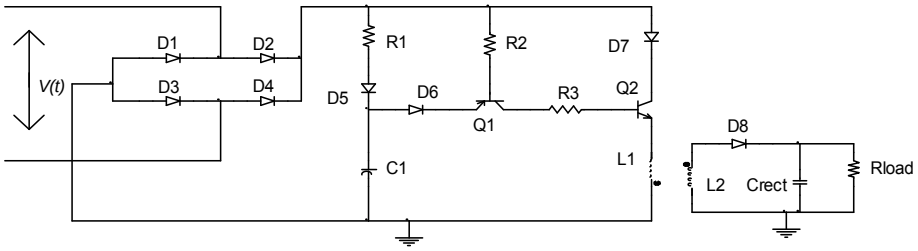

Figure 6. Block diagram of a SCE interface circuit

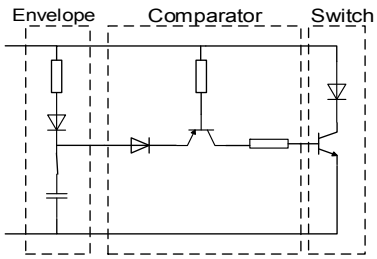

Figure 7. An electronic breaker for maximum displacement

2.3. Non-standard Sinusoidal Signals

Given the development of flow or impact-induced piezoelectric energy harvesting, generated voltage *v(t)* from the piezoelectric energy harvesters is not sinusoidal. Figure 8 and 9 show examples that have no standard sinusoidal excitations. Figure 8 shows the structure of a galloping piezoelectric beam for harvesting wind energy. Figure 9 shows the structure of a rotational piezoelectric wind energy harvester that uses impact-induced resonance. The waveform of *v(t)* is non-standard sinusoidal in some conditions. Figure 10 shows an example waveform of the damped sinusoidal signal of *v(t)* [20, 21]. Figure 11 shows an example waveform of the random signal of *v(t)* [16]. The voltage waveform of *v(t)* as shown in Figure 11

is random but positive because of the rotational piezoelectric wind energy harvesting prototype proposed in [16], which uses impact-induced resonance. In the present simulation analysis, the random signal is assumed to have both positive and negative values. Additionally, the effectiveness of the four aforementioned interface circuits in such situations needs to be determined. Simulation analysis is a fast and convenient way to test the performance of the four interface circuits with non-sinusoidal signals. With reference to the equivalent circuit model for piezoelectric energy harvesters shown in Figure 2 for the simulation analysis, $i_p(t)$ can be set as a damped sinusoidal signal in PSpice and as a random signal in Matlab. Additional details on the simulation are provided in the simulation method section.

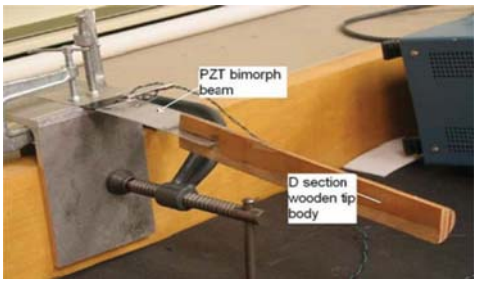

Figure 8. Experimental setup of harvesting wind energy using a galloping piezoelectric beam [20]

Figure 9. Rotational piezoelectric wind energy harvester using impact-induced resonance [16]

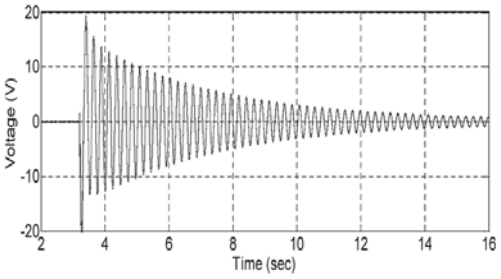

Figure 10. Measured impulse response of the beam with open-circuited electrodes [20]

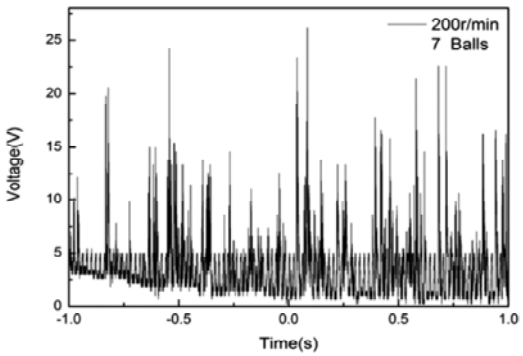

Figure 11. Voltage waveform of the harvester before rectification [16]

3. Simulation Method

The simulation was performed by using OrCAD 16.3/PSpice and Matlab 2012a/Simulink software. PSpice is good for circuit simulation and optimization design, and Matlab performs effectively in system simulation and optimization. The SLPS module in PSpice ensures that the Simulink–Matlab system simulator can be combined with the PSpice circuit simulator. The value of *Cp* in the simulation analysis is 100 *nF*. $i_p(t)$ is discussed in another section. The component models or values for the S-SSHI, P-SSHI, and SCE interface circuits are listed in Table 1, 2, and 3, respectively. The method is introduced together with the damped sinusoidal signals and random signals separately.

Table 1. Component models or values for the S-SSHI interface circuit

Component	Model / Value
R1,R2	100 KΩ
C1,C2	2 nF
Diodes (D1 to D8)	1N4004
PNP transistors (Q1 and Q4)	TIP32C
NPN transistors (Q2 and Q3)	TIP31C
Crect	10 uF
L	47 mH
r	178 Ω

Table 2. Component models or values for the P-SSHI interface circuit

Component	Model/ Value
R1,R6	100 KΩ
R2,R3,R4,R5	10 KΩ
C1,C2	4 nF
Diodes (D1 to D10)	1N4004
PNP transistors (Q1 and Q3)	TIP32C
NPN transistors (Q2 and Q4)	TIP31C
Crect	10 uF
L	47 mH

Table 3. Component models or values for the SCE interface circuit

Component	Model / Value
R1	100 kΩ
R2	51 kΩ
R3	10 kΩ
C1	820 pF
Crect	10 uF
L1,L2	100 mF
Diodes (D1 to D7	1N4004
D8	UF4004

3.1. Damped Sinusoidal Signal

PSpice mainly has six parameters for determining the property of the current source (ISIN), including IOFF, IAMPL, FREQ, PHASE, TD, and DF. The six parameters are defined in Table 4. If *v(t)* is assumed to be sinusoidal, which means that $i_p(t)$ in Figure 2 is assumed to be sinusoidal, then the values of IAMPL and FREQ are set and that of the other parameter becomes the default value of zero. If DF is above zero, *v(t)* becomes a damped sinusoidal voltage waveform as shown in Figure 10. DF is set as 1 in the simulation analysis. The amplitude of $i_p(t)$ is set as 220 uA and the frequency of $i_p(t)$ is set as 2 Hz. The simulation results of the output power with damped sinusoidal signal under certain values and the maximum output power with standard sinusoidal signal are shown in the results section.

Table 4. Definition of the ISIN parameters

Parameter	Definition
IOFF	DC offset current
IAMPL	Amplitude of the current
FREQ	Frequency of the current
PHASE	Initial phase
TD	Delay time
DF	Damping factor

3.2. Random Signal

Random signals can be produced by Matlab–Simulink. Each piezoelectric interface circuit can be in the SLPS module. SL represents Simulink, and PS represents PSpice. The SLPS takes advantages of the two software. Simulink has fast simulation speed and PSpice has high simulation precision. The Simulink model of the equivalent piezoelectric interface circuit

based on the SLPS is shown in Figure 12. A uniform random number replaces the $i_p(t)$ as input parameter of the SLPS, and the scope can show certain output parameters of the SLPS. In the analysis, the scope indicates the output power of the load resistance. The minimum is set as −0.00022 and the maximum is set as 0.00022. The simulation results of the output power under different load resistance values are shown in the results section.

Figure 12. Simulink model of piezoelectric interface circuit based on the SLPS

4. Results

The output power with standard sinusoidal signal can be greatly influenced by the load resistance values except in the SCE interface circuit. The optimal resistance values with standard sinusoidal signals, as well as the output power under optimal resistance values with standard sinusoidal signals and damped sinusoidal signals, are shown in Table 5. The SCE interface circuit has no optimal resistance value and is set as 100 kΩ. With damped sinusoidal signals, the output power can be increased by reducing the load resistance value from the optimal value (Table 5). Given the resistance values with standard sinusoidal signals shown in Table 5, the performance of output power with damped sinusoidal signals is not optimal. Thus, the resistance value with damped sinusoidal signals should be low. The output power with damped sinusoidal signals does not have a constant value. The maximum output power values of certain resistance values are reported in Table 5. As an example, the PSpice results for the output power of the S-SSHI interface circuit with damped sinusoidal signals are shown in Figure 13.

Table 5. Performance of output power with standard sinusoidal and damped sinusoidal signals

Interface circuits	Output power with different signals (mW)	
	Standard sinusoidal signal	Damped sinusoidal signal
SEH	6.09 (900 kΩ)	0.25 (100 kΩ), 0.10(900 kΩ)
S-SSHI	23.82 (400 kΩ)	3.00 (100 kΩ), 1.43 (400 kΩ)
P-SSHI	34.81 (3000 kΩ)	0.24(100 kΩ), 0.003(3000 kΩ)
SCE	16.84 (100 kΩ)	9.11(50 kΩ), 5.36 (100 kΩ)

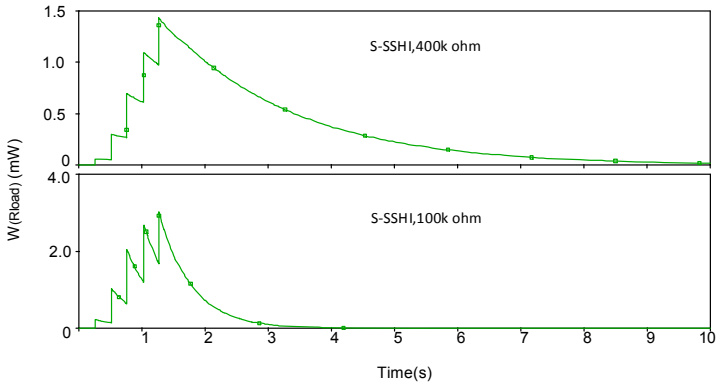

Figure 13. PSpice results for output power of S-SSHI interface circuit with damped sinusoidal signal

For random signals, the Simulink results for output power of different interface circuits are presented in Figure 14. As shown, the performance of the SEH and SCE interface circuits are unsatisfactory. Compared with the other interface circuits, the collected power of the SEH interface circuit is much lower and the collected power of the SCE interface circuit has higher volatility. Thus, when random excitations are exerted on piezoelectric structures, which is a result of the increasing attention on flow- and impact-induced piezoelectric vibration energy harvesting, the P-SSHI and S-SSHI interface circuits may be a good choice for harvesting piezoelectric energy. Meanwhile, the SEH interface circuit has been mostly used in such studies to investigate the performance of certain mechanical structures.

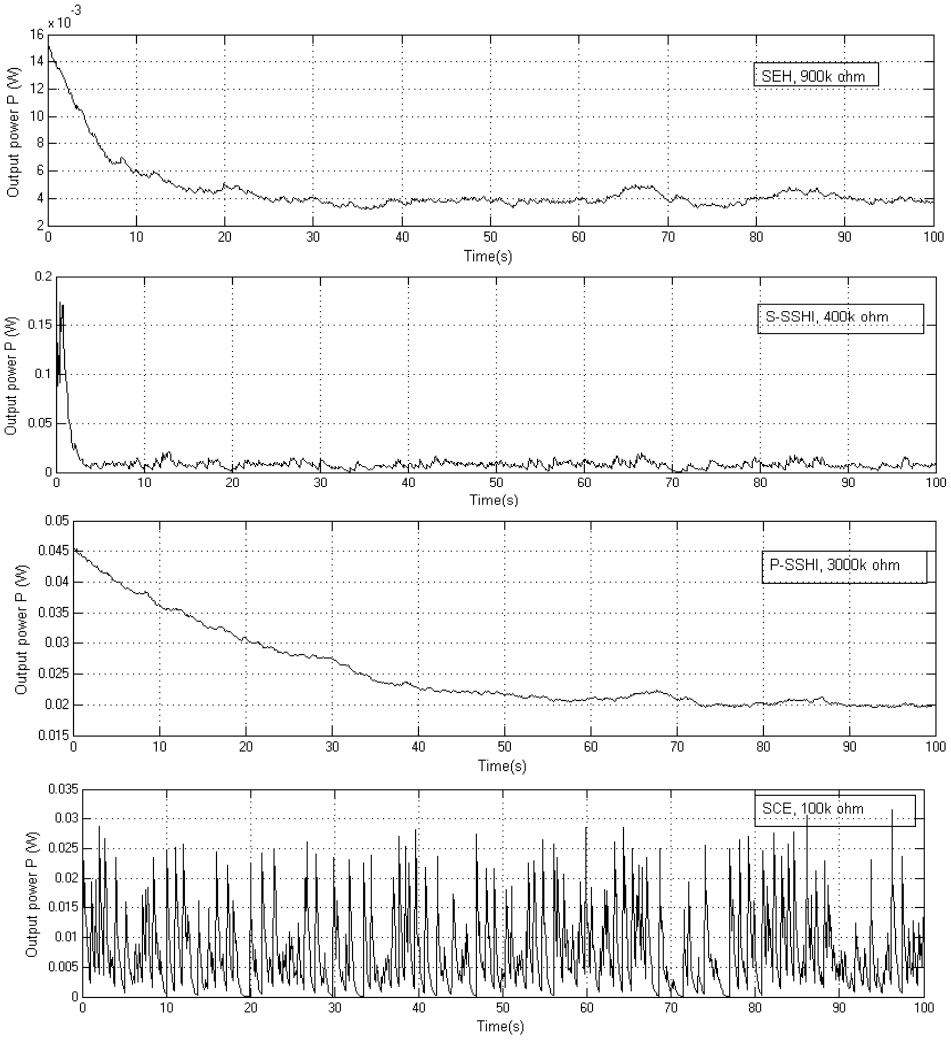

Figure 14. Simulink results for output power of different interface circuits with random signals

5. Conclusion

The performance of different interface circuits with damped sinusoidal signals and random signals was investigated through simulation. Simulation results show that the interface circuits perform effectively under low load resistance values with damped sinusoidal signals, and that the S-SSHI and P-SSHI interface circuits may have improved performance in harvesting piezoelectric energy when constant harmonic excitations are not present. In the future, additional experiments should be conducted to further study the performance of various interface circuits in collecting piezoelectric vibration energy.

Acknowledgements

This work was supported by the National Natural Science Foundation of China (Grant No. 31170669).

References

[1] Chabane F, Moummi N, Benramache S. Experimental analysis on thermal performance of a solar air collector with longitudinal fins in a region of Biskra, Algeria. *Journal of Power Technologies*. 2013; 93(1): 52-58.
[2] Jusoh A, Sutikno T, Guan TK, Mekhilef S. A Review on Favourable Maximum Power Point Tracking Systems in Solar Energy Application. *TELKOMNIKA Telecommunication, Computing, Electronics and Control*. 2014; 12(1): 6-22.
[3] Xu L, Li B. Design of wireless farmland temperature monitoring system based on Zigbee. *Forest Engineering*. 2013; 29(3): 79-82.
[4] Zhang Z, Li WB, Kang JM. Behavior of a thermoelectric power generation device based on solar irradiation and the earth's surface-air temperature difference. *Energy Conversion and management*. 2015; 97: 178-187.
[5] Syafii, Nor KM. Unbalanced Active Distribution Analysis with Renewable Distributed Energy Resources. *TELKOMNIKA Telecommunication, Computing, Electronics and Control*. 2015; 13(1): 21-31.
[6] Liu XJ, Chen RW. Current situation and developing trend of piezoelectric vibration energy harvesters. *Journal of Vibration and Shock*. 2012; 8: 169-176.
[7] Shan XB, Yuan JB, Xie T, Chen WS. Modeling and simulation of power generation with piezoelectric unimorph cantilever. *Journal of Zhejiang University (Engineering Science)*. 2010; 44(3): 528-532.
[8] Park JC, Park JY. Asymmetric PZT bimorph cantilever for multi-dimensional ambient vibration harvesting. *Ceramics International*. 2013; 39: S653-S657.
[9] Chen RW, Ren L, Xia HK, Wang H. Research advance in multi-directional wide-band piezoelectric vibration energy harvesters. *Chinese Journal of Scientific Instrument*. 2014; 35(12): 2641-2652.
[10] He XF, Gao J. Wind energy harvesting based on flow-induced-vibration and impact. *Microelectronic Engineering*. 2013; 111: 82-86.
[11] Zhu L, Chen R, Liu X. Theoretical analyses of the electronic breaker switching method for nonlinear energy harvesting interfaces. *Journal of Intelligent Material Systems and Structures*. 2012; 23: 441-451.
[12] Liang J, Liao WH. Improved design and analysis of self-powered synchronized switch interface circuit for piezoelectric energy harvesting systems. *IEEE Transactions on Industrial Electronics*. 2012; 59: 1950-1960.
[13] Hsieh PH, Chen CH, Chen HC. Improving the scavenged power of nonlinear piezoelectric energy harvesting interface at off-resonance by introducing switching delay. *IEEE Transactions on Power Electronics*. 2015; 30(6): 3142-3155.
[14] Ottman GK, Hofmann HF, Bhatt AC, Lesieutre GA. Adaptive piezoelectric energy harvesting circuit for wireless remote power supply. *IEEE Transactions on Power Electronics*. 2002; 17(5): 669-676.
[15] Sun JC, Chen HJ. Structural design and experimental study on wind-driven piezoelectric generator. *Piezoelectrics & Acoustooptics*. 2012; 34(6): 860-867.
[16] Yang Y, Shen QL, Jin JM, Wang YP, Qian WJ, Yuan DW. Rotational piezoelectric wind energy harvesting using impact-induced resonance. *Applied Physics Letters*. 2014; 105: 053-901.
[17] Ugalde-Caballero CA, Anzurez-Marin J. Low Temperature Thermal Micro Energy Harvester. *DYNA*. 2012; 87(6): 640-646.
[18] Schoeftner J, Buchberger G. A contribution on the optimal design of a vibrating cantilever in a power harvesting application–Optimization of piezoelectric layer distributions in combination with advanced harvesting circuits. *Engineering Structures*. 2013; 53: 92-101.
[19] Lallart M, Lefeuvre É, Richard C, Guyomar D. Self-powered circuit for broadband, multimodal piezoelectric vibration control. *Sensors and Actuators A: Physical*. 2008; 143: 377-382.
[20] Sirohi J, Mahadik R. Harvesting wind energy using a galloping piezoelectric beam. *Journal of Vibration and Acoustics*. 2012; 134: 1-8.
[21] Kwon DS, Ko HJ, Kim MO, Oh Y, Sim J, Lee K, Cho KH, Kim J. Piezoelectric energy harvester converting strain energy into kinetic energy for extremely low frequency operation. *Applied Physics Letters*. 2014; 104: 113-904.